

Supplementary Information

Microfluidic-Based Continuous Flow Formation of Triangular Silver Nanoprisms with Tunable Surface Plasmon Resonance

Michele Carboni, Lorenzo Capretto, Dario Carugo, Eugen Stulz and Xunli Zhang

Effect of pH on the synthesis of silver nanoprisms

In order to assess the effect of pH of the reducing agent solution on NPs formation, experiments were carried out in a batch reactor and UV-Vis-NIR spectra were collected. Silver nanoprisms were synthesized according to the published procedure by Métraux et al,¹ with increasing volumes of 0.01 M basic solution of NaBH₄ added to the final reducing agent solution. As shown in Figure S1, as the volume of the basic solution increases, the optical absorbance moves to shorter wavelengths typical of spherical silver nanoparticles.

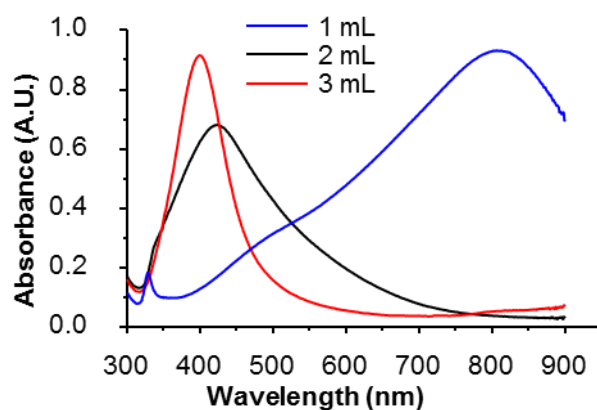


Figure S1. Absorbance spectra acquired for nanoparticles solution prepared by adding different volumes of 0.01 M solution of NaBH₄ to the final reducing solution (final volume 33 mL for all three samples).

Fouling of particles inside the microreactor

In order to verify the effect of the hydrophobic coating in preventing channel fouling, a microfluidic experiment was carried out in a non-functionalized reactor. For monitoring microchannel fouling, microscope images were acquired every 15 minutes by focusing on the channel bottom wall across the channel junction area (i.e. where the three streams joined). As shown in Figure S2a, the grey level intensity inside the channel rises very rapidly as a consequence of NPs precipitation. Figure S2b shows the fouling inside the channel. On the top part small agglomerates of silver are clearly recognizable.

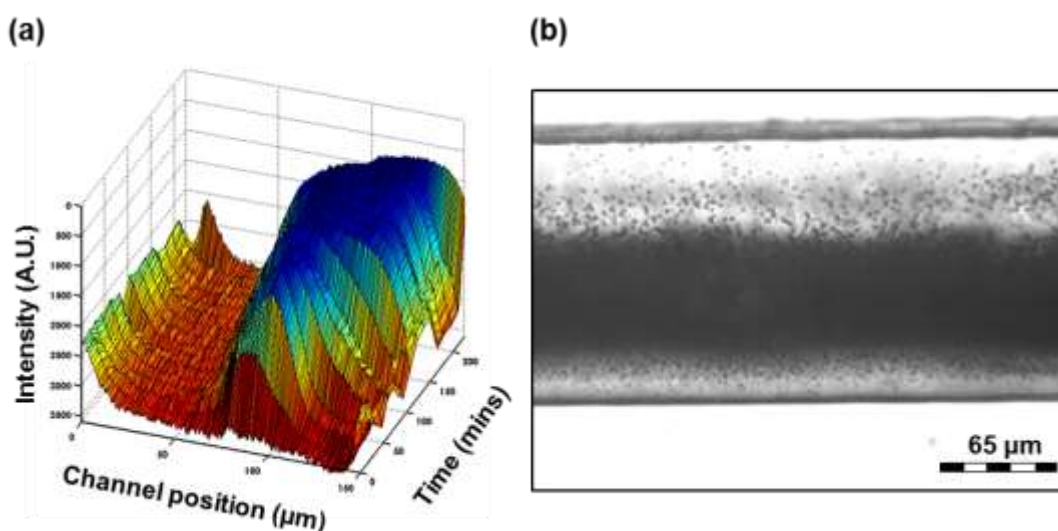


Figure S2. (a) Surface plot showing the temporal evolution of the grey level intensity along the channel. (b) Details of the precipitate are illustrated at higher magnification. Images were acquired using an inverted microscope (IX71, Olympus Corporation, Japan) and a bright field illumination.

Experimental results with microreactors

Experimental results with microreactors shown in Figure 3a and Figure 3b are reported in Table S1 for clarity.

Table S1. Experimental results plotted in Figure 3a and Figure 3b.

R	λ_{\max} (nm)	Edge Length (nm)	FWHM (nm)	Triangles %
0.41	684	17.22	417	84.95
0.44	706	21.67	384	85.92
0.47	720	24.47	364	91.74
0.50	742	29.95	375	88.49
0.54	777	34.11	391	87.78
0.57	799	45.46	468	83.37

Experimental results with microreactors shown in Figure 4a and Figure 4b are reported in Table S2 and Table S3 for clarity.

Table S2. Experimental results plotted in Figure 4a.

R	$V_{\text{tot}}=3.41$ (mL/h)	$V_{\text{tot}}=3.21$ (mL/h)	$V_{\text{tot}}=2.81$ (mL/h)	$V_{\text{tot}}=2.61$ (mL/h)	$V_{\text{tot}}=2.41$ (mL/h)
λ_{\max} (nm)					
0.41	750	766	770	768	777
0.50	750	766	770	781	788
0.57	801	808	794	803	810

Table S3. Experimental results plotted in Figure 4b.

V_{tot} (mL/h)	R=0.41	R=0.50	R=0.57
	FWHM (nm)		
2.41	610	530	504
2.61	595	540	481
2.81	532	524	279
3.01	617	651	487
3.41	708	698	584

Batch synthesis

Experiments using a conventional batch system were also performed for comparison, at the same reagent concentrations employed in the microfluidic-based reactor system. The batch synthesis was carried out using an adapted published procedure.¹ Specifically, TSCD, silver nitrate and H₂O₂ were added in a vial and stirred for 2 minutes before rapidly mixing with a NaBH₄ solution. The concentrations of reagents summarized in Table S4 were chosen to reproduce the concentrations in the microreactor at different V_{tot} (from 3.41 mL/h, Sample 1, to 2.41 mL/h, Sample 6). The resulting changes in the absorbance spectra (spectral position and peak broadness) from the product colloids are illustrated in Figure S3.

Table S4. Concentrations used for batch experiments.

Sample	Concentrations (mM)			
	AgNO ₃	TSCD	H ₂ O ₂	NaBH ₄
1	0.12	2.09	0.047	1.16
2	0.11	2.00	0.045	1.11
3	0.10	1.90	0.043	1.05
4	0.01	1.78	0.040	0.99
5	0.09	1.64	0.037	0.91
6	0.08	1.48	0.033	0.82

Figure S3 shows that the reagent concentrations affected the spectral band position (λ_{max}) and broadness (FWHM), however no clear trend was observed between these parameters. In particular, the spectrum of sample 4 shows an extra narrow and intense peak at about 400 nm indicating a high concentration of spherical particles, which is reflected in a characteristic absorption in that spectral region. The differences between batch and microfluidic systems

suggested that, compared to the bulk solution concentration, the control of the fluid dynamic conditions which governed the mixing process and the chemical microenvironment played a crucial role for the production of nanoparticles with tunable characteristics.

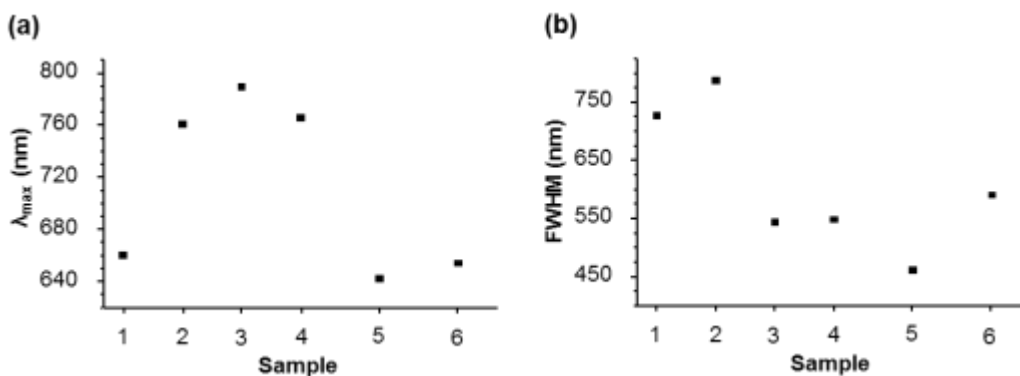


Figure S3. (a) λ_{\max} and (b) FWHM at different reagent concentrations, as reported in Table S1.

TEM Images

Transmission electron microscopy (TEM) images of nanoparticles were acquired with an FEI Technai12 TEM by drop casting 10 μ L of colloid solution on sample grids (S160-4 Carbon Films on 3 mm 400 mesh grids), and imaging at acceleration potential of 120 kV. Figure S5 shows TEM images of particles synthesized at different flow rates (from 3.41 mL/h, Figure S5a, to 2.41 mL/h, Figure S5f).

TEM image analysis was carried out with an in house developed Matlab code (The Mathworks Inc., USA) allowing to determine three key parameters, namely, minimum Feret diameter (ω), maximum circumscribed circles radius (C_R) and particle area (A), which were employed in previous studies to characterize the shape of particles and calculate the edge length of the

triangles.² After quantification of ω , C_R and A , the particle's equilateral triangularity (ET) and roundness (RD) were calculated by using Eqs. (1) & (2).²

$$ET = \frac{\omega}{\sqrt{3A}} \quad (1)$$

$$RD = \frac{A}{\pi C_R^2} \quad (2)$$

When $ET > 0.6$ and $0.1 < RD < 0.5$, the particles were identified as triangular, according to Rivollier et al.² Furthermore, in this range of ET and RD values, triangles are mostly equilateral or isosceles. Once the triangular shaped particles were identified among all particles examined, their edge lengths were calculated as the Feret diameter (d), which corresponds to the maximum edge length and thus to the maximum distance between two points in a triangular shape. ET and RD calculated for sample prepared under different flow conditions are shown in Figure S5

Table S5. Edge length distribution for particles synthesized at different R.

Edge Length (nm)	R=0.41 Count	R=0.44 Count	R=0.47 Count	R=0.50 Count	R=0.54 Count	R=0.57 Count
0	0	0	0	0	0	0
10	54	22	0	4	1	0
20	208	130	205	85	53	16
30	69	85	101	146	146	93
40	42	38	55	66	92	73
50	18	11	22	37	40	74
60	6	5	11	15	14	39
70	2	0	4	16	14	18
80	0	0	0	4	8	6
90	0	1	0	1	4	11
100	0	0	1	0	3	6
110	0	0	0	1	1	10
120	0	0	0	1	2	2

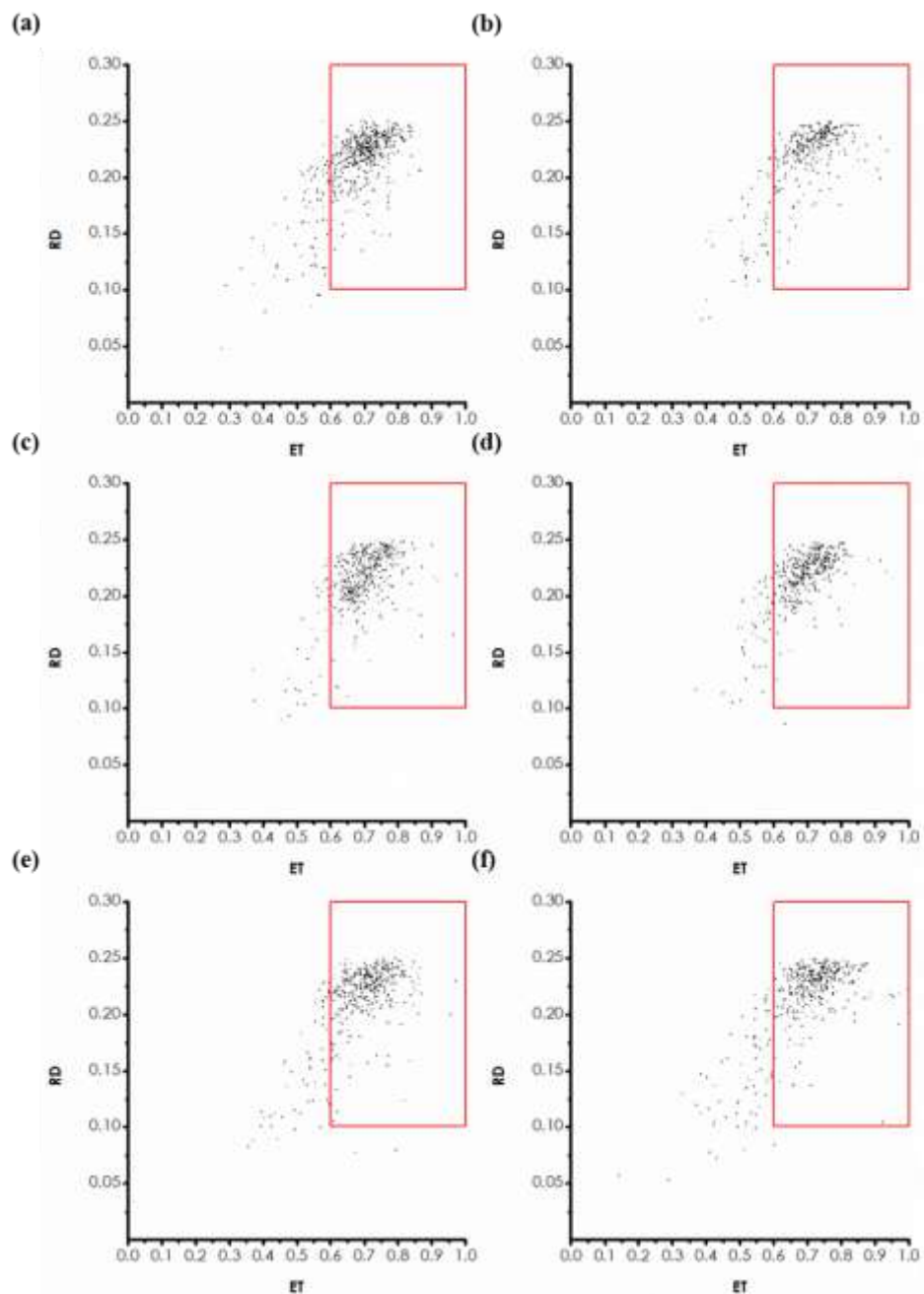


Figure S4. *RD* vs *ET* plotted for silver nanoprisms synthesis at different flow rates (a) 3.41 mL/h, (b) 3.21 mL/h, (c) 3.01 mL/h, (d) 2.81 mL/h, (e) 2.61 mL/h, (d) 2.41 mL/h.

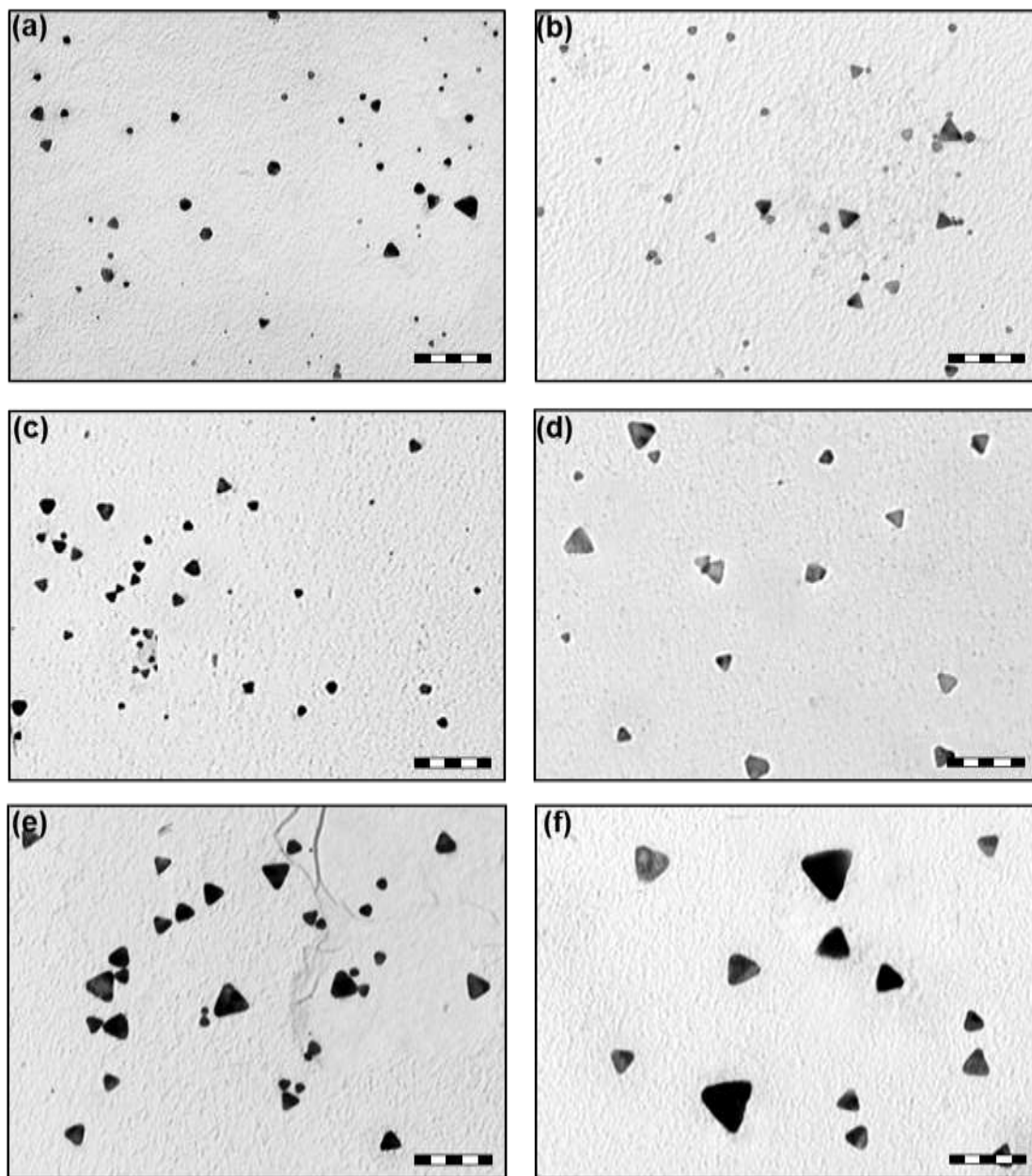


Figure S5. TEM images of silver nanoprisms at different flow rates (a) 3.41 mL/h, (b) 3.21 mL/h, (c) 3.01 mL/h, (d) 2.81 mL/h, (e) 2.61 mL/h, (d) 2.41 mL/h. The scale bar is 200 nm for all pictures.

References

1. G. S. Métraux and C. A. Mirkin, *Advanced Materials*, 2005, **17**, 412-415.
2. S. Rivollier, J. Debayle and J. Pinoli, in *Image Processing Theory Tools and Applications (IPTA) 2010*, pp. 411-416.